Lawrence Berkeley National Laboratory
Lawrence Berkeley National Laboratory

Title
Non-magnetic compensation in ferromagnetic Ga1-xMnxAs and Ga1-xMnxP synthesized by ion implantation and pulsed-laser melting

Permalink
https://escholarship.org/uc/item/3h23k3g2

Author
Scarpulla, M.A.

Publication Date
2008-12-16

Non-magnetic compensation in ferromagnetic $Ga_{1-x}Mn_xAs$ and $Ga_{1-x}Mn_xP$ synthesized by ion implantation and pulsed-laser melting

M.A. Scarpulla, P.R. Stone, I.D. Sharp, E.E. Haller, and O.D. Dubon

Department of Materials Science & Engineering, University of California, Berkeley, CA 94720 and

Lawrence Berkeley National Laboratory, Berkeley, CA 94720

J.W. Beeman and K.M. Yu

Lawrence Berkeley National Laboratory, Berkeley, CA 94720

ABSTRACT

The electronic and magnetic effects of intentional compensation with non-magnetic donors are investigated in the ferromagnetic semiconductors $Ga_{1-x}Mn_xAs$ and $Ga_{1-x}Mn_xP$ synthesized using ion implantation and pulsed-laser melting (II-PLM). It is demonstrated that compensation with non-magnetic donors and Mn_I have similar qualitative effects on materials properties. With compensation T_C decreases, resistivity increases, and stronger magnetoresistance and anomalous Hall effect attributed to skew scattering are observed. $Ga_{1-x}Mn_xAs$ can be controllably compensated with Te through a metal-insulator transition through which the magnetic and electrical properties vary continuously. The resistivity of insulating $Ga_{1-x}Mn_xAs:Te$ can be described by thermal activation to the mobility edge and simply-activated hopping transport. $Ga_{1-x}Mn_xP$ doped with S is insulating at all compositions but shows decreasing T_C with compensation. The existence of a ferromagnetic insulating state in $Ga_{1-x}Mn_xAs:Te$ and $Ga_{1-x}Mn_xP:S$ having T_Cs of the same order as the uncompensated materials demonstrates

that localized holes are effective at mediating ferromagnetism in ferromagnetic semiconductors through the percolation of ferromagnetic 'puddles' which at low temperatures.

Email: mikes@engr.ucsb.edu, oddubon@berkeley.edu

Current address for M.A. Scarpulla: Materials Department, University of California Santa Barbara, Santa Barbara, CA 93106.

INTRODUCTION

Ferromagnetism in $Ga_{1-x}Mn_xAs$ and $Ga_{1-x}Mn_xP$ random alloys containing no second phases is mediated by holes introduced by the substitutional Mn_{Ga} acceptors [1,2]. The fact that Mn_{Ga} provides both magnetic moments and holes in these ferromagnetic semiconductors (FMSs) mandates that the manipulation of additional electronic defects is necessary to decouple the magnetic moment and hole concentrations. Therefore, the complete understanding of the hole-mediated ferromagnetic phase in these materials requires independent experimental variation of both the hole and Mn concentrations.

Control of carrier concentration in III-Mn-V FMSs has been previously achieved through manipulation of residual defects from thin film epitaxy. $Ga_{1-x}Mn_xAs$ grown by low-temperature molecular beam epitaxy (LT-MBE) is heavily compensated in the as-grown state by interstitial Mn_I. It has been demonstrated that post-growth annealing can eliminate these defects, which are believed to be double donors, thus providing a route to controlling the carrier concentration. Ion-channeling demonstrated conclusively that interstitial Mn_I was the defect responsible for the compensation [3,4]. Although the simultaneous effects induced by low-temperature post-growth annealing on the ferromagnetically-participating Mn and hole concentrations have been considered theoretically [5], it is still desirable to perform experiments where the hole and magnetic moment concentrations may be altered independently to elucidate the physics of these III-V ferromagnetic semiconductors.

Isolation of the effect of hole concentration on the ferromagnetic and electrical properties of $Ga_{1-x}Mn_xAs$ and $Ga_{1-x}Mn_xP$ from the magnetic moment concentration can be achieved through co-doping with an additional electrically-active element. In $Ga_{1-x}Mn_xAs$ it has been shown that for low Mn concentrations ($x \leq 0.03$) additional holes can be introduced by adding Be acceptors [6,7]. However, for $Ga_{1-x}Mn_xAs$ it is not possible to increase the hole concentration above a certain level corresponding to approximately $x=0.05$ by co-doping with shallow acceptors [3,8]. Therefore, a greater dynamic range of carrier concentrations for all x may be accessed through compensation of holes by addition of a non-magnetic donor. Efforts have been made in this direction in LT-MBE $Ga_{1-x}Mn_xAs$ at low Mn concentration ($x=0.013$) using Sn [9] and more recently for $x=0.085$ over a wide range of hole concentrations using Te [6,10]. Passivation of Mn acceptors with hydrogen has also been used to suppress the hole concentration in $Ga_{1-x}Mn_xAs$ [11-13] and in $Ga_{1-x}Mn_xP$ [14].

Ion implantation and pulsed laser melting (II-PLM) is an established technique for achieving extremely-high doping concentrations in semiconductors. It was originally investigated due to the ability to incorporate and activate traditional dopants in semiconductors at concentrations in the 10^{21} /cm^3 range – levels difficult to achieve even in advanced growth techniques such as metalorganic chemical vapor deposition (MOCVD) and MBE. Research in this area is still active in Si, where high concentrations of group III and V dopants (e.g. P, As, Sb, In, Bi) can be activated for use in ultra-shallow transistor structures [15-18]. Research on traditional dopants in III-V materials is not as active, but very similar results have been achieved demonstrating doping concentrations in the 10^{20}-10^{21} /cm^3 range in GaAs doped with Se and Te using

II-PLM [19-21]. Our group has successfully applied II-PLM to the synthesis of III-Mn-V ferromagnetic semiconductors [2,22-24].

In this work, we have investigated intentionally compensated $Ga_{1-x}Mn_xAs$:Te and $Ga_{1-x}Mn_xP$:S synthesized by II-PLM. Epitaxial films grown by II-PLM are well-suited for such an investigation into intentionally-compensated III-Mn-V materials for two reasons. First, the high temperatures during II-PLM associated with melting and solidification preclude the presence of Mn_I [23], which would complicate experiments if present. Second, it is simple to incorporate large concentrations of multiple dopants via sequential ion implantation steps [22,25].

EXPERIMENTAL

For the experiments in $Ga_{1-x}Mn_xAs$:Te, (001)-oriented semi-insulating GaAs wafers were implanted at 7° from the surface normal with 160 keV Te^+ at doses ranging from 1.9×10^{15} to 1.1×10^{16} cm^{-2} and then with 80 keV Mn^+ to 1.84×10^{16} cm^{-2}. These implants produce an amorphous layer of approximately 60 nm thick. The ion energies were chosen in order to match the projected range of the two species at ~50 nm. Implantation of Te before Mn is critical due to the high sputtering rate of Te which would otherwise result in varying Mn concentrations with Te dose. Samples approximately 5 mm on a side were cleaved from the implanted wafers producing <110> edges. Each sample was irradiated in air at a fluence of 0.2 or 0.4 J/cm^2 with a single pulse from a KrF excimer laser (λ = 248 nm) having duration ~32 ns, FWHM 23 ns, and peak intensity at

16 ns. The film properties are uniform across each sample as the laser pulses passed through a crossed-cylindrical lens homogenizer which produced a very uniform spatial intensity distribution of ±5 % and heat flow during film solidification occurs only in the perpendicular direction as the melted region is typically only 100 nm thick.

For $Ga_{1-x}Mn_xAs$:Te, 0.2 J/cm^2 is sufficient to melt through the amorphous layer while 0.4 J/cm^2 corresponds to melting through the additional ion-damage which extends further into the sample. Accordingly, the Rutherford backscattering spectrometry (RBS) ion channeling from films irradiated at 0.4 J/cm^2 indicate better crystalline quality than films irradiated at 0.2 J/cm^2. After irradiation, the total amounts of both Mn and Te are lower due to solute redistribution during PLM; the retained Mn dose measured with particle induced X-ray emission (PIXE) was 1.3x10^{16} /cm^2 for 0.2 J/cm^2 and 1.1x10^{16} /cm^2 for 0.4 J/cm^2 due to the different solidification velocities during PLM. The level of Te compensation will be discussed in terms of implanted Te dose as data for the retained Te dose was not available for all samples and the degree of compensation may vary significantly with depth. The substitutional fractions f_{subs} of Mn and Te were measured using RBS and PIXE channeling analysis; the Mn f_{subs} was approximately 65-70% for all films while the Te f_{subs} was 90-100 %. For reference to our previous work, in Ref. [22] the sample identified as γ=0.64 was implanted with 5.6x10^{15} Te/cm^2 and the sample identified as γ=0.96 was implanted with 1.1x10^{16} Te/cm^2.

For the experiments in $Ga_{1-x}Mn_xP$:S, 50 keV Mn$^+$ was implanted to 1.5x10^{16} /cm^2 followed by 60 keV S$^+$ to doses between 1.0x10^{15} and 7.3x10^{15} cm^{-2}. The retained dose of S was not measurable using RBS/PIXE because of the overlap between the

characteristic X-rays from S and P. $Ga_{1-x}Mn_xP:S$ samples were irradiated at 0.44 J/cm^2, which is sufficient to melt through the entire ion-damaged region.

Film magnetization was measured with a SQUID magnetometer along in-plane <110> directions using a field of 50 Oe for temperature-dependent measurements. $Ga_{1-x}Mn_xAs$ implanted at 50 keV to $1.5x10^{16}$ $/cm^2$ and irradiated at 0.3 J/cm^2 exhibits saturation magnetization of 3.2 ± 0.3 μ_B per total Mn, corresponding to 4.3 ± 0.4 μ_B per substitutional Mn_{Ga} [24], which is in excellent agreement with the best measurements from LT-MBE grown $Ga_{1-x}Mn_xAs$ [26,27]. For $Ga_{1-x}Mn_xP$ with x=0.042, a moment of 3.9 ± 0.4 μ_B/Mn_{Ga} was reported [2]. T_C estimations were made by extrapolating the steepest portion of the temperature-dependent data to zero magnetization and are reported herein with an uncertainty of 2-3 K caused by sample-to-sample variation. For some samples where the substitutional fraction of Mn was not available, the magnetization data is reported in emu/g Mn, where the total amount of Mn (Mn_{Ga} and non-commensurate Mn) was determined from the sample area and non-channeled PIXE measurements.

Etching $Ga_{1-x}Mn_xAs$ films in concentrated HCl for 5-20 minutes removed excess Mn from the surface that was present in Ga-rich droplets and in surface oxides. Etching $Ga_{1-x}Mn_xP$ films in concentrated HCl for 24 hours additionally removes a highly-twinned surface layer [2,25]. It was verified that these etch processes did not affect the ferromagnetic properties of either type of film, however removing the highly-twinned layer from $Ga_{1-x}Mn_xP$ allowed electrical contact to be made to the ferromagnetic layer – the 300 K sheet resistivity decreased from ~10^5 to 10^4 $\Omega/\square$ upon etching samples having x=0.042 and temperature-dependent changes were measurable [2]. Magnetotransport measurements were made with the field applied perpendicular to the sample plane and in

the van der Pauw geometry using cold-pressed indium contacts on the corners of the samples. These simple contacts are Ohmic at all temperatures for $Ga_{1-x}Mn_xAs$ and compensated $Ga_{1-x}Mn_xAs$:Te films as evaluated by I-V curves taken at each temperature and field combination. Ohmic behavior was observed down to 10 K for the pressed-indium contacts on $Ga_{0.958}Mn_{0.042}P$ samples [2]; however contacts to more insulating $Ga_{1-x}Mn_xP$ films having lower Mn_{Ga} concentration or compensated with Te or S became non-Ohmic at low temperatures. Data reported herein were measured within the regime of Ohmic behavior. Field symmetrization was used to isolate the Hall signal from even-symmetry components of the magnetoresistance.

RESULTS & DISCUSSION

A. Resistivity in $Ga_{1-x}Mn_xAs$:Te

Figure 1 presents the sheet resistivity of the two series of $Ga_{1-x}Mn_xAs$:Te samples irradiated at 0.2 and 0.4 J/cm^2. Panels (a) and (b) of Fig. 1 present the data as ρ_{sheet} vs. $1/T$ while panels (c) and (d) present the logarithm of the same data vs. T mapped onto the interval 0 to 1 in order to accentuate the anomalies associated with T_C. As all of the samples are strictly insulating at very low temperatures, we use the functional definition that metallic samples have a region below T_C where the resistivity decreases with decreasing temperature. In both sample series, the films change gradually from metallic to insulating with the metal-insulator transition (MIT) being very near the sample implanted with 5.6×10^{15} /cm^2 Te for the 0.2 J/cm^2 series and somewhere below this dose

for the 0.4 J/cm^2 series. The shapes of the curves change gradually from the behavior of metallic Ga$_{1-x}$Mn$_x$As having a magnetic scattering peak associated with T$_C$ to curves having a shoulder near T$_C$ to curves where scattering effects at T$_C$ are not readily apparent [1,28-30]. This is consistent with scattering effects becoming less dominant as the transport mode changes from band-like to thermally-activated hopping. This behavior appears to be general in Ga$_{1-x}$Mn$_x$As and indicative of carrier localization whether by lower Mn content [1], compensation by Mn$_I$ [31,32], or compensation by non-magnetic donors [6,10]. The fact that the 0.4 J/cm^2 films are more insulating for a given Te dose reflects the lower amount of Mn retained. Comparing the uncompensated and 5.6x10^{15} /cm^2 Te samples in both series to the data for low-temperature annealed Ga$_{1-x}$Mn$_x$As in [33] indicates that the presence of Mn$_I$ and Te appear to be very similar in their effects on the temperature dependent resistivity. This is surprising due to the large Mn$_I$ moment; however this may be confirmation of the predicted weak *p-d* coupling expected for Mn$_I$ [34] which would mitigate the effects of Mn$_I$ on hole transport beyond reduction of the hole concentration.

Despite most reports on Ga$_{1-x}$Mn$_x$As reporting Mott variable-range hopping (T$^{-1/4}$) for insulating or dirty metallic samples at low temperatures [35-37] the linear behavior in Fig. 1 panels (a) and (b) indicate simply-activated (T^{-1}) behavior for all samples down to 4.2 K. T^{-1} hopping gave better agreement than either T$^{-1/4}$ or T$^{-1/2}$ over the measured temperature range; however other behavior may be present in an even lower temperature regime. The low-temperature activation energies range from 0.07 meV for the 0.2 J/cm^2 7.5x10^{15} Te/cm^2 sample to 2.2 meV for the 0.2 J/cm^2 7.5x10^{15} Te/cm^2 sample. Simply-activated T^{-1} hopping is predicted by the percolation models of Kaminski and Das Sarma

[29] and is conceptually consistent with the "puddle" description of Shklovskii and Efros [38] for highly doped and compensated conventional semiconductors (when magnetic effects are taken into account) and the magnetoimpurity description of Nagaev [39]. The magnetoimpurity scattering model has been applied in both the ferromagnetic and paramagnetic regimes [7,40] for more metallic samples near T_C and the *p-d* exchange energies thus extracted are in good agreement with those from the spin-disorder scattering models typically applied [41]. Note that magnetoimpurity scattering is not a good description for insulating films; scaling theories such as that by Zarand *et al.* [30] are more applicable but unfortunately do not allow physical parameter extraction.

For insulating samples near the MIT (e.g. the 0.2 J/cm^2 samples and the 0.4 J/cm^2 5.6x10^{15} Te/cm^2 sample), the Arrhenius plots exhibit two regimes having nearly-linear behavior. If the high-temperature regime is interpreted as being due to thermal activation, the different slopes are representative of different activation energies, as is the case for $Ga_{1-x}Mn_xP$ [2]. For more highly insulating samples of $Ga_{1-x}Mn_xAs$:Te and $Ga_{1-x}Mn_xP$, a gradual curvature over the measurable range with no anomaly at T_C is observed rather than two distinct regimes. Note that the change in slope, which is associated with T_C for insulating samples of $Ga_{1-x}Mn_xAs$:Te and $Ga_{1-x}Mn_xP$ very near the MIT, is distinct from the change in hopping activation energy discussed in Ref. [29] unless T_C is identical to T_{cover}, the temperature corresponding to the percolation threshold of bound magnetic polarons (in Ref. [29], $T_{cover} << T_C$). In $Ga_{1-x}Mn_xAs$:Te and $Ga_{01-x}Mn_xP$ with x>0.042 the change in slope of the resistivity is strongly associated with T_C. For $Ga_{1-x}Mn_xP$ samples with x<0.042, T_C occurs at temperatures below the change in dominant thermally-activated transport mechanism. Similar to our claim for $Ga_{1-x}Mn_xP$, we propose that the

change in slope associated with T_C in $Ga_{1-x}Mn_xAs$:Te is due to a change in the dominant transport mechanism. In $Ga_{1-x}Mn_xP$, we attribute the high-temperature thermally-activated transport process to thermal activation across an energy gap separating the Mn impurity band from the valence band [2]. In $Ga_{1-x}Mn_xAs$:Te, however, an impurity band separated from the valence band by an energy gap is not expected although the details of the bandstructure appear to be very complex [42].

$Ga_{1-x}Mn_xAs$:Te with $0.02<x$ should be an Anderson localized system, where no gap exists in the density of states but the disorder caused by compensation localizes some states [43]. Thermally-activated transport with a small activation energy corresponding to activation of carriers from E_F to the mobility edge (E_m) has been used to describe transport in non-magnetic Anderson-localized systems [44]. For the case of hole transport, the resistivity near the MIT is given by

$$\frac{1}{\rho} \propto k_B T \ln\left\{1 + \exp\left(\frac{E_m - E_F}{k_B T}\right)\right\}$$

(Eq. 1)

where (E_m-E_F)<0 indicates that E_F resides within localized states. A similar model also including the effects of phonon scattering was used to describe $Ga_{1-x}Mn_xAs$ in [37], although 2nd phase precipitation may have occurred due to the relatively high annealing temperatures used. Such a phonon scattering contribution was not necessary to fit the current data.

In $Ga_{1-x}Mn_xP$, infrared photoconductivity and transport provide evidence for a gap in the density of states of 25–75 meV for $x \approx 0.03$–0.042 separating the Mn impurity band from the valence band [2]. Thermal activation across this energy gap produces a very similar temperature dependent resistivity at high temperatures; however at low

temperatures this resistivity would continue to rise while the behavior described by Eq. 1 saturates. In both $Ga_{1-x}Mn_xP$ and $Ga_{1-x}Mn_xAs$:Te hopping conduction dominates at low temperatures and adding an additional T^{-1} hopping term attributed to the hopping of magnetic polarons or, equivalently, to holes hopping between puddles allows the entire temperature range for samples of $Ga_{1-x}Mn_xAs$:Te to be fit using

$$\frac{1}{\rho} = Ak_BT \ln\left\{1 + \exp\left(\frac{E_m - E_F}{k_BT}\right)\right\} + B\exp\left\{\frac{-E_{hop}}{k_BT}\right\} \qquad \text{(Eq. 2)}$$

where A and B are constants and (E_m-E_F) and E_{hop} are the activation energies for the two thermally-activated processes.

Figure 2 depicts the temperature dependent resistivity of the four most insulating $Ga_{1-x}Mn_xAs$:Te samples for which no scattering peak near T_C is present along with the best fits to the model. The values for the hopping and (E_m-E_F) activation energies are noted for each data set. It is apparent that this model can accurately describe the resistivity behavior of insulating $Ga_{1-x}Mn_xAs$:Te for which magnetic scattering effects at T_C are not dominant. We find that (E_m-E_F) is nearly constant at 6.0±0.4 meV for the samples irradiated at 0.2 J/cm^2 while for the sample irradiated at 0.4 J/cm^2, this activation energy is 11.8 meV. In $Ga_{1-x}Mn_xAs$, higher laser fluences result in films with lower Mn concentration; however how fluence affects the compensation ratio in this case is not fully understood. The low-temperature hopping energy is sensitive to the degree of compensation, as is demonstrated by the three samples irradiated at 0.2 J/cm^2 and having E_{hop} varying from 0.22 – 2.04 meV with increasing Te compensation.

A recent work [45] has proposed assigning the *high-temperature* (T>T_C) dependence of resistivity in low-doped $Ga_{1-x}Mn_xAs$ with x<0.015 to variable range hopping and has

related the associated characteristic temperature with T_C. For very low compositions below an extrapolated value of x~0.01, the Mn impurity band does merge with the valence band [43], unlike the case for the $Ga_{1-x}Mn_xAs$:Te discussed herein where the large Mn composition would ensure the merged impurity band.

B. Magnetotransport in $Ga_{1-x}Mn_xAs$:Te

Figure 3 shows the field dependence of magnetoresistance for a $Ga_{1-x}Mn_xAs$:Te sample implanted with 160 keV Te to 5.6×10^{15} /cm^2 and irradiated at 0.2 J/cm^2 and having T_C very close to 96 K while Fig. 4 displays the Hall resistance for the same sample. The shapes and qualitative behavior of both of these quantities are nearly identical to those for uncompensated $Ga_{1-x}Mn_xAs$ [24]; however their magnitude is substantially larger in both cases. It can be seen that the negative MR is stronger by a factor of approximately 2-3 in the Te-compensated sample, in line with the expectation for MR due to spin scattering. Similarly, the magnitude of the saturated Hall resistance for the Te compensated sample is roughly a factor of 5 larger than that from the $Ga_{1-x}Mn_xAs$ sample discussed in Ref. [24]. Equation 2 gives the dependence of the Hall resistance on the sheet resistivity (R_{sheet}) for the case where the anomalous Hall effect (AHE) dominates the normal component [46]

$$R_{Hall} \cdot t \propto R_{sheet}^{\alpha} \cdot M \qquad \text{(Eq. 3)}$$

Here, R_{Hall} is the Hall resistance, t is the film thickness, M is the magnetization, and $\alpha=1$ for skew scattering and $\alpha=2$ for side-jump scattering. Knowing that the effective film thicknesses are roughly the same for the $Ga_{1-x}Mn_xAs$ and $Ga_{1-x}Mn_xAs$:Te films, the larger

R_{sheet} of the $Ga_{1-x}Mn_xAs$:Te sample (~1300 $\Omega/\square$ at 5 K) compared to the $Ga_{1-x}Mn_xAs$ sample (~380 $\Omega/\square$ at 5 K) can account for the larger R_{Hall} observed. It is also possible to make a rough estimate of α in $Ga_{1-x}Mn_xAs$ from these two data sets noting that Te is a non-magnetic scattering center and will thus not contribute to the AHE. Assuming full saturation of the magnetization at 5 K and 50 kOe and using the magnetizations for both samples measured using SQUID magnetometry (200 emu/g Mn and 180 emu/g Mn respectively) and the magnitudes of R_{Hall} at low temperatures (80 Ω and 16 Ω respectively) yield an estimate of 1.2 for α. This is in good agreement with previous results indicating skew scattering as the origin of the AHE in $Ga_{1-x}Mn_xAs$ [1].

C. Magnetization in $Ga_{1-x}Mn_xAs$:Te

Figure 5 presents the temperature-dependent magnetization of the two series of $Ga_{1-x}Mn_xAs_{1-y}Te_y$ samples implanted with differing Te doses and irradiated at 0.2 or 0.4 J/cm^2. As the samples vary gradually from metallic to insulating the curvature of the temperature-dependent magnetization changes sign. Nearly linear curves are found for samples near the MIT. Such changes in convexity are a general prediction of most models of the magnetization of a system consisting of local moments interacting through carriers via an exchange interaction [47-51]. The continuous transition in curvature through the MIT taken with the similar continuous change in resistivity demonstrates that the hole-mediated ferromagnetic phase exists over a range of carrier localization. This gives insight into the mechanism of ferromagnetic exchange and requires that a full theory of these ferromagnetic semiconductors span both the band-like and localized carrier regimes.

D. Magnetization in $Ga_{1-x}Mn_xP$:S

Temperature-dependent magnetization data for a series of $Ga_{1-x}Mn_xP_{1-y}S_y$ samples with differing S implant doses are shown in Figure 6. The magnetization of all samples shows a nearly linear-dependence on the temperature due to the more localized nature of the carriers in the wider gap $Ga_{1-x}Mn_xP$ system. As expected for a carrier-mediated phase T_C decreases monotonically with increasing compensation of ferromagnetism-mediating holes. This observation is consistent with X-ray magnetic circular dichroism measurements taken at the Mn $L_{3,2}$ absorption edges, which shows a decrease in the spin polarization of the carriers at the Fermi level with increasing S concentration [52]. The extremely-high resistivity of these films and/or poor contacts has so far precluded measuring their temperature dependent transport down to low temperatures.

CONCLUSIONS

The properties of intentionally compensated thin films of $Ga_{1-x}Mn_xAs$:Te and $Ga_{1-x}Mn_xP$:S synthesized using II-PLM have been presented. It is demonstrated that the effects of intentional doping with shallow donors are similar to the effects of compensation by Mn_I in $Ga_{1-x}Mn_xAs$. The T_C of both types of films decreases with compensation, accompanied by more insulating behavior. The increasing resistivity is

accompanied by stronger magnetoresistivity and anomalous Hall effect attributed to skew scattering.

Intentionally compensated ferromagnetic $Ga_{1-x}Mn_xAs$:Te and $Ga_{1-x}Mn_xP$:S correspond to the 'highly doped and compensated semiconductors' described by Shklovskii and Efros [38] with the addition of a strong *p-d* exchange energy. The smooth variation of magnetic and transport properties through the MIT, when taken with the results from $Ga_{1-x}Mn_xP$, indicates that holes localized to a small number of Mn ions are also capable of mediating ferromagnetism in III-Mn-V ferromagnetic semiconductors. The localization in these cases is believed to occur by the spontaneous formation of 'puddles' of holes that couple the surrounding Mn_{Ga} ions ferromagnetically [29,38,47]. Hopping between these puddles in turn couples them to each other.

In both the temperature dependencies of resistivity and magnetization of $Ga_{1-x}Mn_xAs_{1-y}Te_y$ samples, gradual and continuous transitions are seen as the carrier concentration is reduced through the MIT. The characteristics associated with magnetic scattering of band-like states gradually become less pronounced and are replaced with temperature dependencies associated with hopping of localized carriers between localized states. However, while the carrier concentration in delocalized valence band-like states is drastically reduced, the effects on T_C are not nearly as pronounced. In passing from a dirty metallic system characterized by delocalized hole states and T_C ~130 K to a system with localized states at E_F and T_C of 50-70 K there is at most a factor of 3 change in T_C. Similarly, in moving from $Ga_{1-x}Mn_xAs$ to $Ga_{1-x}Mn_xP$ while keeping the Mn_{Ga} composition approximately constant, there is a change from delocalized valence band-

like holes to holes localized in an impurity band, while the T_C similarly decreases by only a factor of ~2 to 60 K.

These observations indicate that carrier-mediated ferromagnetism of comparable magnetic properties can exist in III-Mn-V systems for a continuum of carrier localization. Indeed, it is stated quite explicitly in Ref. [53] and in careful readings of Refs. [51,54] that this continuum of localization should be acknowledged in theoretical understandings of the physics of these systems and that 'somewhat-localized' holes are also effective in mediating exchange. Similar conclusions have been reached in computational work [55,56]. $Ga_{1-x}Mn_xP$ with x up to 0.042 provides a limiting case of exchange mediated by impurity band carriers. Although it is conceptually convenient to regard the carriers as either localized in an impurity band or delocalized in valence band states, the real situation in III-Mn-Vs such as $Ga_{1-x}Mn_xAs$ and $In_{1-x}Mn_xAs$ is not so well defined and should be regarded as intermediate between these extremes.

REFERENCES

[1]   H. Ohno, Science **281,** 951 (1998).

[2]   M. A. Scarpulla, B. L. Cardozo, R. Farshchi, W. M. H. Oo, M. D. McCluskey, K. M. Yu, and O. D. Dubon, Physical Review Letters **95,** 207204 (2005).

[3]   K. M. Yu, W. Walukiewicz, T. Wojtowicz, W. L. Lim, X. Liu, U. Bindley, M. Dobrowolska, and J. K. Furdyna, Physical Review B **68,** 041308 (2003).

[4]   K. M. Yu, W. Walukiewicz, T. Wojtowicz, I. Kuryliszyn, X. Liu, Y. Sasaki, and J. K. Furdyna, Physical Review B **65,** 201303 (2002).

[5]   G. Bouzerar, T. Ziman, and J. Kudrnovsky, Physical Review B **72,** 125207 (2005).

[6]   P. K. Khabibullaev and S. U. Yuldashev, Journal of Communications Technology and Electronics **50,** 1038 (2005).

[7]   S. U. Yuldashev, H. Im, V. S. Yalishev, C. S. Park, T. W. Kang, S. Lee, Y. Sasaki, X. Liu, and J. K. Furdyna, Applied Physics Letters **82,** 1206 (2003).

[8]   K. M. Yu, W. Walukiewicz, T. Wojtowicz, W. L. Lim, X. Liu, M. Dobrowolska, and J. K. Furdyna, Applied Physics Letters **84,** 4325 (2004).

[9]   Y. Satoh, D. Okazawa, A. Nagashima, and J. Yoshino, Physica E **10,** 196 (2001).

[10]   S. U. Yuldashev, H. C. Jeon, H. S. Im, T. W. Kang, S. H. Lee, and J. K. Furdyna, Physical Review B **70,** 193203 (2004).

11   S. T. B. Goennenwein, T. A. Wassner, H. Huebl, M. S. Brandt, J. B. Philipp, M. Opel, R. Gross, A. Koeder, W. Schoch, and A. Waag, Physical Review Letters **92,** 227202 (2004).

12   L. Thevenard, L. Largeau, O. Mauguin, A. Lemaitre, and B. Theys, Applied Physics Letters **87,** 182506 (2005).

13   R. Bouanani-Rahbi, B. Clerjaud, B. Theys, A. Lemaitre, and F. Jomard, Physica B-Condensed Matter **340,** 284 (2003).

14   C. Bihler, M. Kraus, M. S. Brandt, S. T. B. Goennenwein, M. Opel, M. A. Scarpulla, R. Farshchi, D. M. Estrada, and O. D. Dubon, *Submitted* (2008).

15   A. Herrera-Gomez, P. M. Rousseau, G. Materlik, T. Kendelewicz, J. C. Woicik, P. B. Griffin, J. Plummer, and W. E. Spicer, Applied Physics Letters **68,** 3090 (1996).

16   D. Nobili, A. Carabelas, G. Celotti, and S. Solmi, Journal of the Electrochemical Society **130,** 922 (1983).

17   Y. Takamura, S. H. Jain, P. B. Griffin, and J. D. Plummer, Journal of Applied Physics **92,** 230 (2002).

18   C. W. White, in *Pulsed Laser Processing of Semiconductors*; *Vol. 23*, edited by R. F. Wood, C. W. White, and R. T. Young (Academic Press, Orlando, Fla., 1984), p. 44-92.

[19]   P. A. Barnes, H. J. Leamy, J. M. Poate, S. D. Ferris, J. S. Williams, and G. K. Celler, Applied Physics Letters **33,** 965 (1978).

[20]   J. A. Golovchenko and T. N. C. Venkatesan, Applied Physics Letters **32,** 147 (1978).

[21]   J. S. Williams, in *Laser annealing of semiconductors*, edited by J. M. Poate and J. W. Mayer (Academic Press, New York, 1982), p. 383-435.

[22]   M. A. Scarpulla, K. M. Yu, W. Walukiewicz, and O. D. Dubon, AIP Conference Proceedings **772,** 1367 (2005).

[23]   M. A. Scarpulla, O. D. Dubon, K. M. Yu, O. Monteiro, M. R. Pillai, M. J. Aziz, and M. C. Ridgway, Applied Physics Letters **82,** 1251 (2003).

[24]   M. A. Scarpulla, R. Farshchi, P. R. Stone, Y. Suzuki, O. D. Dubon, R. V. Chopdekar, and K. M. Yu, Journal of Applied Physics**,** *In Press* (2007).

[25]   M. A. Scarpulla, U. Daud, K. M. Yu, O. Monteiro, Z. Liliental-Weber, D. Zakharov, W. Walukiewicz, and O. D. Dubon, Physica B **340,** 908 (2003).

[26]   K. W. Edmonds, N. R. S. Farley, T. K. Johal, G. van der Laan, R. P. Campion, B. L. Gallagher, and C. T. Foxon, Physical Review B **71,** 064418 (2005).

[27]   T. Jungwirth, K. Y. Wang, J. Masek, K. W. Edmonds, J. Konig, J. Sinova, M. Polini, N. A. Goncharuk, A. H. MacDonald, M. Sawicki, A. W. Rushforth, R. P. Campion, L. X. Zhao, C. T. Foxon, and B. L. Gallagher, Physical Review B **72,** 165204 (2005).

[28]   M. E. Fisher and J. S. Langer, Physical Review Letters **20,** 665 (1968).

[29]   A. Kaminski and S. Das Sarma, Physical Review B **68,** 235210 (2003).

[30]   G. Zarand, C. P. Moca, and B. Janko, Physical Review Letters **94,** 247202 (2005).

[31]   I. Kuryliszyn, T. Wojtowicz, X. Liu, J. K. Furdyna, W. Dobrowolski, J. M. Broto, M. Goiran, O. Portugall, H. Rakoto, and B. Raquet, Acta Physica Polonica A **102,** 659 (2002).

[32]   S. J. Potashnik, K. C. Ku, R. Mahendiran, S. H. Chun, R. F. Wang, N. Samarth, and P. Schiffer, Physical Review B **66,** 012408 (2002).

[33]   K. W. Edmonds, K. Y. Wang, R. P. Campion, A. C. Neumann, N. R. S. Farley, B. L. Gallagher, and C. T. Foxon, Applied Physics Letters **81,** 4991 (2002).

[34]   J. Blinowski and P. Kacman, Physical Review B **67,** 121204 (2003).

[35]   Y. Iye, A. Oiwa, A. Endo, S. Katsumoto, F. Matsukura, A. Shen, H. Ohno, and H. Munekata, Materials Science and Engineering B **63,** 88 (1999).

[36]   S. Katsumoto, T. Hayashi, Y. Hashimoto, Y. Iye, Y. Ishiwata, M. Watanabe, R. Eguchi, T. Takeuchi, Y. Harada, S. Shin, and K. Hirakawa, Materials Science and Engineering B **84,** 88 (2001).

[37]   A. van Esch, L. van Bockstal, J. DeBoeck, G. Verbanck, A. S. van Steenbergen, P. J. Wellmann, B. Grietens, R. Bogaerts, F. Herlach, and G. Borghs, Physical Review B **56,** 13103 (1997).

38   B. I. Shklovskii and A. L. Efros, *Electronic Properties of Doped Semiconductors* (Springer, Berlin, 1984).

39   E. L. Nagaev, *Colossal Magnetoresistance and Phase Separation in Magnetic Semiconductors* (Imperial College Press, London, 2002).

40   S. T. B. Goennenwein, S. Russo, A. F. Morpurgo, T. M. Klapwijk, W. Van Roy, and J. De Boeck, Physical Review B **71,** 193306 (2005).

41   F. Matsukura, H. Ohno, A. Shen, and Y. Sugawara, Physical Review B **57,** R2037 (1998).

42   K. S. Burch, D. B. Shrekenhamer, E. J. Singley, J. Stephens, B. L. Sheu, R. K. Kawakami, P. Schiffer, N. Samarth, D. D. Awschalom, and D. N. Basov, Physical Review Letters **97,** 087208 (2006).

43   T. Jungwirth, J. Sinova, A. H. MacDonald, B. L. Gallagher, V. Novak, K. W. Edmonds, A. W. Rushforth, R. P. Campion, C. T. Foxon, L. Eaves, E. Olejnik, J. Masek, S. R. E. Yang, J. Wunderlich, C. Gould, L. W. Molenkamp, T. Dietl, and H. Ohno, Physical Review B **76,** 125206 (2007).

44   M. A. Dubson and D. F. Holcomb, Physical Review B **32,** 1955 (1985).

45   B. L. Sheu, R. C. Myers, J. M. Tang, N. Samarth, D. D. Awschalom, P. Schiffer, and M. E. Flatte, Physical Review Letters **99,** 227205 (2007).

46   C. L. Chien and C. R. Westgate, *The Hall Effect and Its Applications* (Plenum Press, New York, 1980).

47   A. Kaminski and S. Das Sarma, Physical Review Letters **88,** 247202 (2002).

48   S. Das Sarma, E. H. Hwang, and A. Kaminski, Physical Review B **67,** 155201 (2003).

49   C. Timm, F. Schafer, and F. von Oppen, Physical Review Letters **89,** 137201 (2002).

50   M. Berciu and R. N. Bhatt, Physical Review B **69,** 045202 (2004).

51   T. Dietl, H. Ohno, and F. Matsukura, Physical Review B **6319,** 195205 (2001).

52   P. R. Stone, M. A. Scarpulla, R. Farshchi, I. D. Sharp, J. W. Beeman, K. M. Yu, E. Arenholz, J. D. Denlinger, E. E. Haller, and O. D. Dubon, AIP Conf. Proc. **893,** 1177 (2007).

53   H. Kepa, L. Van Khoi, C. M. Brown, T. Dietl, J. K. Furdyna, and T. M. Giebultowicz, Physica B **350,** 36 (2004).

54   T. Dietl, H. Ohno, F. Matsukura, J. Cibert, and D. Ferrand, Science **287,** 1019 (2000).

55   P. Mahadevan and A. Zunger, Applied Physics Letters **85,** 2860 (2004).

56   K. Sato, P. H. Dederichs, H. Katayama-Yoshida, and J. Kudrnovsky, Journal of Magnetism and Magnetic Materials **272-76,** 1983 (2004).

FIGURE CAPTIONS

Figure 1 – Temperature dependent ρ_{sheet} for a series of $Ga_{1-x}Mn_xAs$:Te films irradiated at (a) 0.2 and (b) 0.4 J/cm^2. Panels (c) & (d) present the normalized logarithm of the same data to accentuate the shapes of the curves. Arrows indicate T_C for each sample. Both series of samples encompass a metal-insulator transition and the associated disappearance of an anomaly near T_C associated with magnetic scattering.

Figure 2 – (points) ρ_{sheet} vs. inverse temperature for the four most insulating $Ga_{1-x}Mn_xAs$:Te samples. Fits to the transport model including hopping and thermal activation processes are shown as lines. The extracted hopping activation energy and (E_m-E_F) activation energy are indicated near the high- and low-temperature regions (respectively) of each curve in meV.
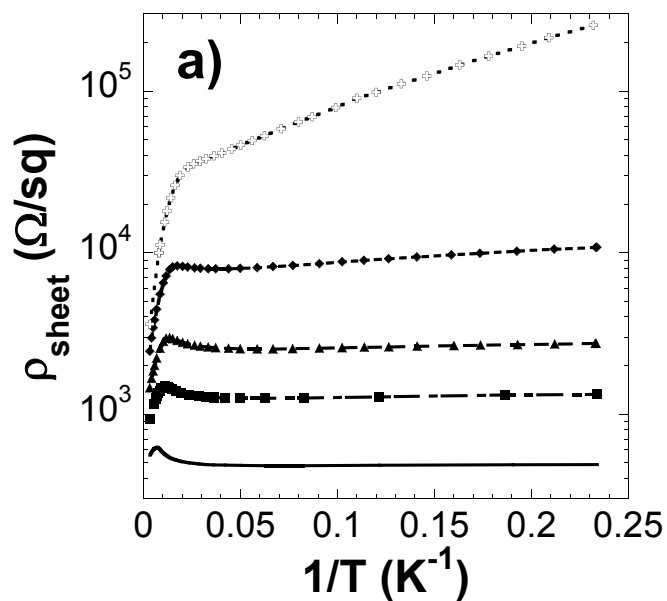
Figure 3 – Field-dependent magnetoresistance at different temperatures for a sample of $Ga_{1-x}Mn_xAs$:Te having a T_C of 96 K. The data above T_C is shown as dotted lines.

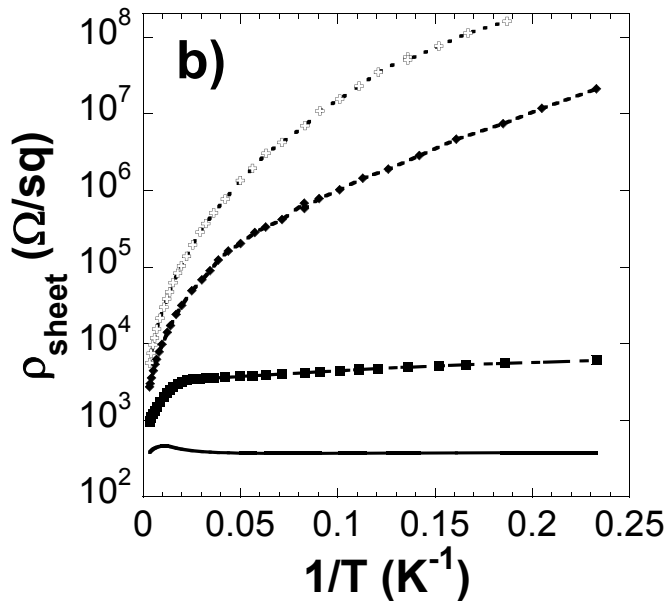**Figure 4** – Hall resistance at 5 K as a function of field for the sample in Fig. 3.

Figure 5 – Normalized temperature-dependent magnetization for the two series of $Ga_{1-x}Mn_xAs$:Te films presented in Fig. 1. The metal-insulator transition is accompanied by a continuous change in concavity; linear magnetization curves are characteristic of samples close to the MIT.

Figure 6 – Temperature-dependent magnetization for a series of $Ga_{1-x}Mn_xP:S$ films. An increase in the concentration of S donors is accompanied by a drop in T_C.
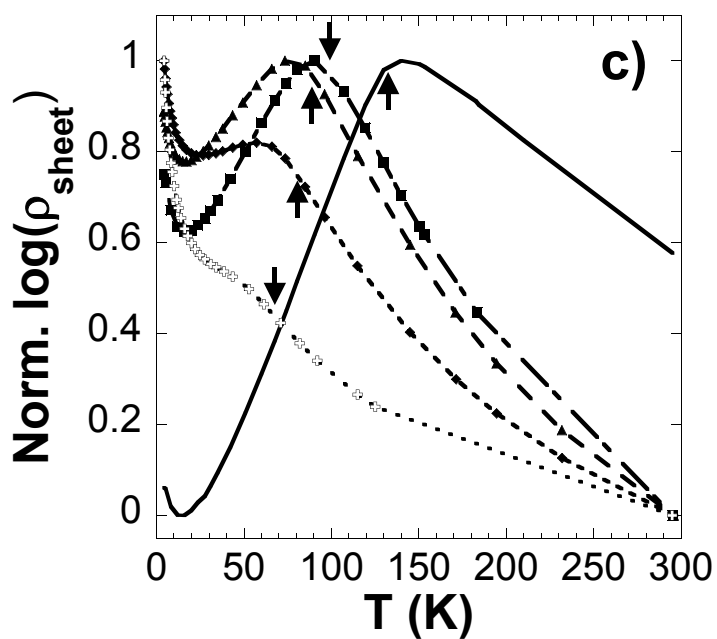
0.2 J/cm² a)

0.4 J/cm² b)
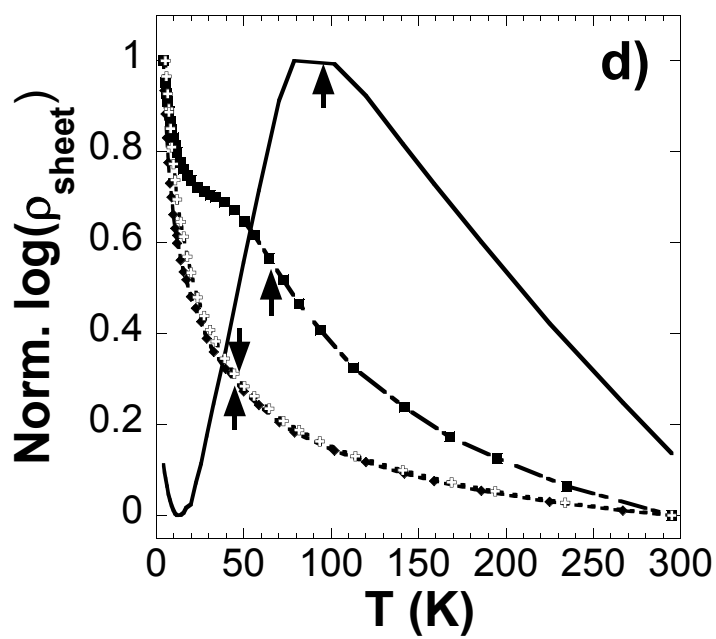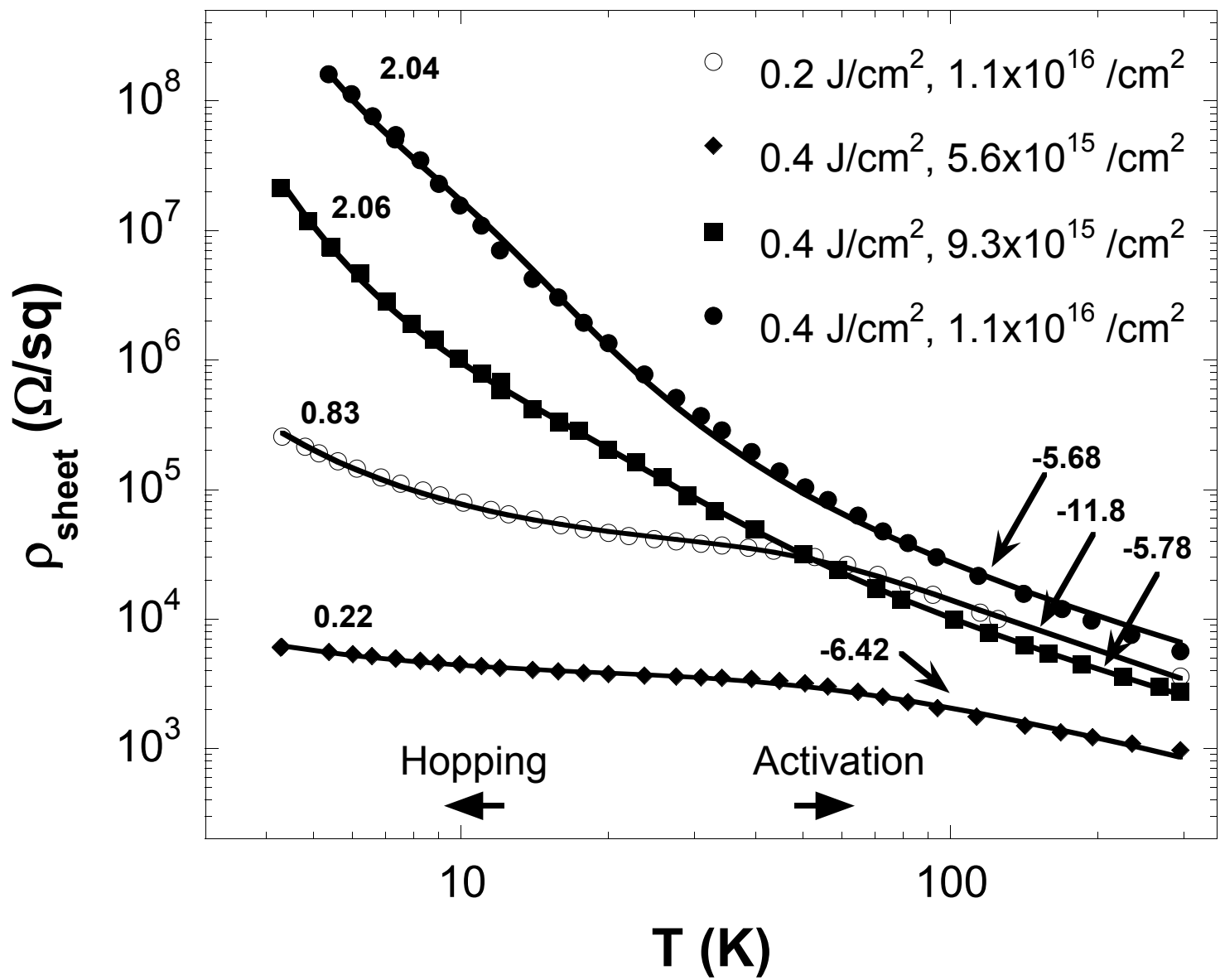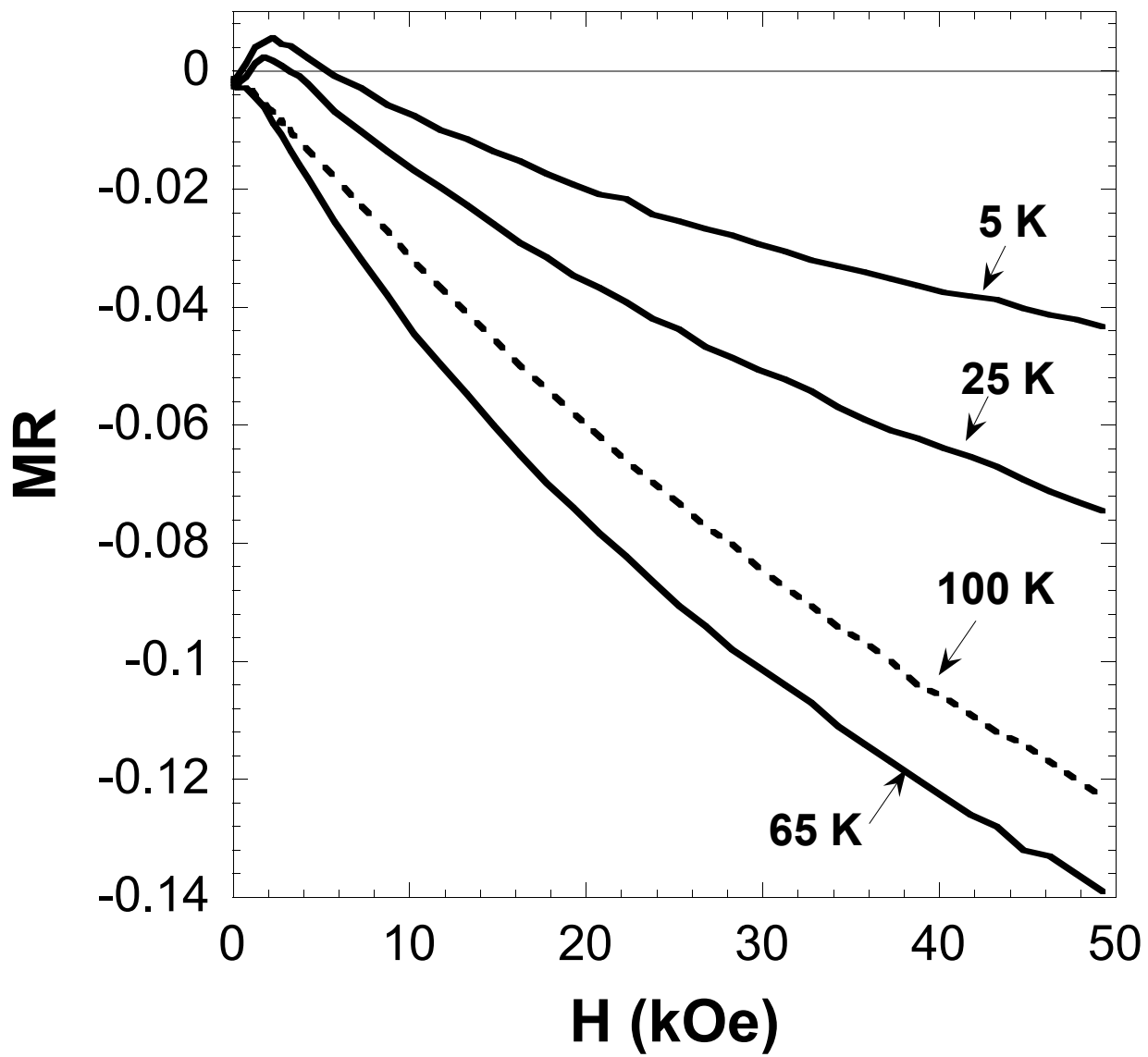
Mn Only 9.3x10¹⁵
5.6x10¹⁵ 1.1x10¹⁶
7.5x10¹⁵

Mn Only 9.3x10¹⁵
5.6x10¹⁵ 1.1x10¹⁶

0.2 J/cm² c)

0.4 J/cm² d)

0.2 J/cm²

Legend:
- Mn Only
- 1.9×10^{15} /cm²
- 5.6×10^{15} /cm²
- 7.5×10^{15} /cm²
- 9.3×10^{15} /cm²
- 1.1×10^{16} /cm²

(a)

0.4 J/cm²

Legend:
- Mn Only
- 3.7×10^{15} /cm²
- 7.5×10^{15} /cm²
- 9.3×10^{15} /cm²
- 1.1×10^{16} /cm²

(b)

Axis labels: M / M(5 K) versus T (K)